SCIENTIFIC REPORTS

OPEN

SUBJECT AREAS:
NANOWIRES
COLLOIDS
NANOSCALE MATERIALS

Received
11 September 2013

Accepted
24 October 2013

Published
11 November 2013

Correspondence and requests for materials should be addressed to X.Y.S. (xshi@dhu.edu.cn) or X.-Q.G. (xgong@ecust.edu.cn)

Dendrimer-mediated hydrothermal synthesis of ultrathin gold nanowires

Hui Liu[1,2], Xiaoming Cao[3], Jianmao Yang[1,4], Xue-Qing Gong[3] & Xiangyang Shi[1,2,5]

[1]State Key Laboratory for Modification of Chemical Fibers and Polymer Materials, Donghua University, Shanghai 201620, People's Republic of China, [2]College of Chemistry, Chemical Engineering and Biotechnology, Donghua University, Shanghai 201620, People's Republic of China, [3]State Key Laboratory of Chemical Engineering, Centre for Computational Chemistry and Research Institute of Industrial Catalysis, East China University of Science and Technology, Shanghai 200237, People's Republic of China, [4]Research Center for Analysis & Measurement, Donghua University, Shanghai 201620, People's Republic of China, [5]CQM-Centro de Química da Madeira, Universidade da Madeira, Campus da Penteada, 9000-390 Funchal, Portugal.

We report the use of poly(amidoamine) dendrimers as stabilizers to synthesize ultrathin Au nanowires (NWs) with a diameter of 1.3 nm via a hydrothermal approach. The formation of uniform Au NWs was optimized by varying the Au/Ag salt molar ratio, dendrimer stabilizers, and reaction solvent, temperature, and time. A novel growth mechanism involving a synergic facet-dependent deposition/reduction of Ag(I) and oriented migration of Au atoms is proposed based on density functional theory calculations and the experimental results. This work can significantly expand the scope of dendrimers as stabilizers to generate metal NWs in aqueous solution that may be further functionalized for different applications.

One-dimensional metal nanostructures have continuously attracted considerable interest due to their unique properties derived from the high aspect ratio and their potential applications in the areas including but not limited to catalysis[1], electronics[2,3], sensors[4–6], and photonics[7]. Several different synthetic approaches, such as nanoparticle (NP) assembly[8–10], surfactant-directed growth[11,12], polymer templating[13,14], and electrodeposition[15], have been employed to prepare metal nanowires (NWs), especially Au NWs. However, under most of the circumstances, ultrathin Au NWs with a diameter range of 1–5 nm are not able to be generated, which is largely due to the lack of the transverse growth control of the Au NWs. When approaching the nanometer scale, the ultrathin Au NWs are expected to have improved electronic and quantum size-dependent properties that can be further exploited for many interesting applications.

In 2007, Halder and Ravishankar launched the synthesis of ultrathin single-crystalline Au NWs despite the limitation in purity and synthesis protocol[8]. In 2008, ultrathin single-crystalline Au NWs were reported independently by four research groups with improved synthesis methods[2,16–18]. In their effort to synthesize ultrathin Au NWs with a diameter fallen into a range of 1.8–3.0 nm along the growth direction of <111>, oleylamine (OA) has been commonly used as a stabilizing agent, and organic solvents such as hexane and chloromethane have been employed in most cases[17–20]. The use of organic solvents may generate environmental hazard, limiting the application of the synthesized ultrathin Au NWs, especially in biomedical applications. Therefore, development of novel and green route to synthesize Au NWs in aqueous solution still remains a great challenge.

In our previous work, we have shown that amine-terminated generation 5 poly(amidoamine) (PAMAM) dendrimer ($G5.NH_2$) enables the shape evolution of Au-Ag alloy from NPs to NWs[21]. Unlike the usual role played as template or stabilizer in the synthesis of spherical metal NPs[22–25], dendrimer is able to mediate the growth of Au-Ag alloy NWs in the presence of Ag(I) ions at room temperature. However, under the studied conditions, the formed Au-Ag NWs with a diameter of 3.7 nm have a quite large diameter distribution and the formation mechanism is still unclear. This prior work suggests that dendrimers may be able to replace the role played by OA, allowing for the formation of Au NWs in aqueous solution. With the advantage of tunable surface modification, dendrimers can be easily functionalized to exhibit desirable properties[26–28], possibly leading to the formation of multifunctional NW structures. This should be much more advantageous than those synthetic approaches undertaken in organic medium at high temperatures using OA as stabilizing agent[2,8].

In this report, ultrathin Au NWs with a mean diameter of 1.3 nm and length up to micrometer scale were prepared through a facile hydrothermal approach in the presence of dendrimers. A wide range of synthetic parameters such as reaction time, temperature, solvent, and additive were systematically investigated to explore their effects on the formation of Au NWs. In addition, a new insight into the growth mechanism was proposed by density functional theory (DFT) calculations and confirmed by further experimental results.

Results

At the Au/Ag/G5 dendrimer molar feed ratio of 15/5/1 in a water bath of 40°C, Au NWs were able to be formed in aqueous solution. UV-Vis spectrometry was used to monitor the growth process of Au NWs (Supplementary Fig. S1). At 4 h time point, an obvious absorption peak appeared at around 500 nm with almost no absorption in the near-infrared region. With the reaction time, the peak around 500 nm exhibited a red-shift to 510 nm (8 h) and 520 nm (12 h and later) with enhanced absorbance in near-infrared region. The peak around 500 nm can be attributed to the surface plasmon resonance (SPR) band of spherical Au NPs[29], and the red-shifted peaks (520 nm) with the reaction time can be assigned to the transverse SPR band of Au NWs[11]. The corresponding longitudinal SPR band of the NWs should be in the far infrared region due to the micrometer-length of the NWs[11].

TEM was performed to confirm the growth process of Au NWs (Fig. 1). At the 8 h time point (Fig. 1a), mixture of spherical Au NPs and Au nanorods were formed. With the reaction time, Au NWs were formed with less and less spherical Au NPs and Au nanorods (Fig. 1b–d). After 48 h, NWs with uniform morphology were formed with a diameter of 1.3 nm and length up to micrometer scale (Fig. 1e–f and Supplementary Fig. S2). After 48 h, the morphology of the NWs seems to be stable and does not show much difference till 72 h (Supplementary Fig. S3). The composition of the Au NWs at different time points was analyzed by ICP-OES (Supplementary Table S1).

The role of Ag(I) ions in the NW formation was investigated by regulating the Au/Ag molar feed ratios (Supplementary Fig. S4). Clearly, no NWs are formed in the absence of $AgNO_3$ in this reaction protocol (Supplementary Fig. S4a). At the Au/Ag molar ratio of 15/2.5, mixture of irregular nanorods and spherical NPs are formed (Supplementary Fig. S4b). Addition of excess amount of $AgNO_3$ (Au/Ag molar ratio of 15/7.5) was not beneficial for the generation of uniform NWs (Supplementary Fig. S4c). Therefore, the optimized Au/Ag molar feed ratio was selected to be 15/5. Further, the unique role of directing the NW growth played by Ag(I) ions cannot be replaced by other nitrates. By replacing $AgNO_3$ with $NaNO_3$, only spherical or hemi-spherical NPs can be formed under similar experimental conditions (Supplementary Fig. S5). Moreover, the morphology of the products is also dependent on the generation of the dendrimers. As opposed to G5 dendrimers, the use of low generation dendrimers (e.g. G3.NH_2) was not able to afford the generation of regular uniform Au NWs (Supplementary Fig. S6). Furthermore, the morphology of Au NWs is dependent on the dendrimer surface functionalization. By acetylating the dendrimer surface amines according to our previous study[21] and confirmed by ^{1}H NMR spectroscopy (Supplementary Fig. S7), the diameter of the NWs was increased from 1.3 nm to 2.0 nm and some curly rods appeared (Fig. 2).

To study the growth orientation of the NWs, high-resolution TEM was performed. The images of NWs after acetylation clearly show the crystal lattice structure (Fig. 3). The NWs seem to grow along the <111> direction. Interestingly, two different {111} crystal facets were found. One is parallel to the growth direction (Fig. 3a) and the other is in 55° deviation from the growth direction (Fig. 3b). The latter one can be found in the literature[30] and the presence of

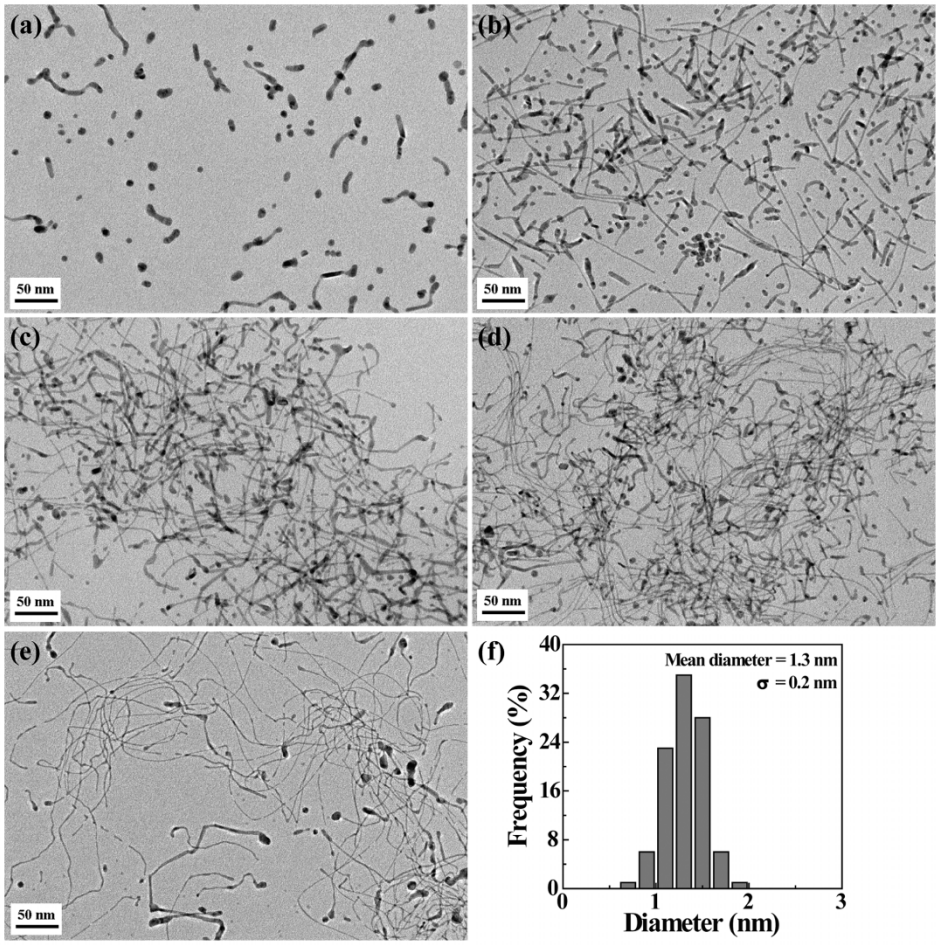

Figure 1 | The growth process of the NWs investigated by TEM. TEM images of samples taken at 8 h (a), 12 h (b), 24 h (c), 36 h (d), and 48 h (e), respectively in the process of NW formation. The NWs were hydrothermally prepared using Au/Ag/G5 dendrimer molar feed ratio at 15/5/1 in a water bath of 40°C. (f) shows the diameter distribution histogram of the NWs formed at 48 h.

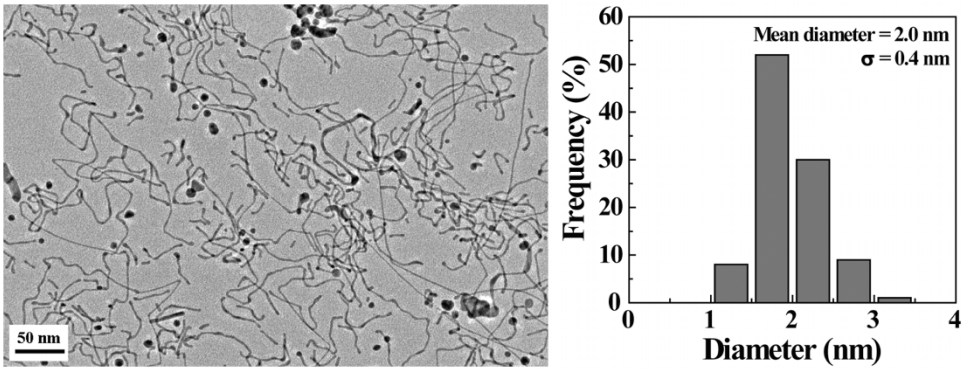

Figure 2 | The morphology of the acetylated NWs. TEM image and diameter distribution histogram of the NW product after acetylation of the NWs shown in Figure 1e.

Ag may lead to a slight shift of the crystal lattice when compared to the pure Au case[17,31]. The former is rarely seen, which may remain within the NWs during the shape evolution process (Supplementary Fig. S8). Detailed mechanistic exploration is required for further clear understanding.

For Ag-assisted Au NWs[17] and Au-Ag bimetallic NWs[30], the exact role played by Ag is still unclear. Aiming at understanding the growth mechanism of Au NWs, we carried out DFT calculations to explore the role played by $AgNO_3$. According to our experimental results, only Au NPs or short Au nanorods can be formed and there is almost no Ag existing in these particles at the first 8 h. This suggests that Ag(I) ions could be reduced following their adsorption on the Au NP surfaces. Hence, a perfect face-centered cubic (FCC) octahedral Au_{38} cluster model was selected on which (100) and (111) surfaces are exposed[32]. Due to the limitation of the used simulation software, this model does not include the stabilization role played by dendrimers. However, given the important role played by Ag in directing the NW growth (Supplementary Fig. S4 and Fig. S5), we deem that the established model is sufficient to illustrate the NW growth mechanism. As illustrated in Supplementary Fig. S9a, the surface atoms at Au(100) display more negative net charge than those at Au(111), which could be attributed to their low-coordination numbers. This makes the surface atoms at Au(100) capable of attracting certain amount of cations. Therefore, one may expect that Ag(I) ions prefer to adsorb onto Au(100) rather than Au(111) crystal facet. In fact, our calculated adsorption energies also show that Ag atom binds with Au(100) more strongly: the adsorption energies of Ag atom on (100) and (111) of Au_{38} are 5.84 and 5.23 eV, respectively. Accordingly, we may expect that {100} can be readily deposited by Ag during the growth process of the NWs.

To take into consideration of surface defects in the realistic system, we also calculated an $Au_{37}Ag$ particle based on the octahedral Au_{38} model in which one Ag atom adsorbs on the defect site of a missing Au. It can be found that the adsorbed Ag tends to migrate to the subsurface of Au NP, which can be attributed to the fact that Au is more stable than Ag and by replacing Ag at the exposed facets it can stabilize the whole NP (Fig. 4). Furthermore, it is intriguing to note that the net charges of surface Au atoms adjacent to the subsurface of Ag are even more negative than those adjacent to Au (Supplementary Fig. S9b). This is clearly due to the higher electronegativity of Au than that of Ag, so that surface Au atoms bonding to Ag can take more cations. This indicates that the surface area around subsurface Ag can attract more Ag(I) ions after it is incorporated into Au NPs. Hence, a strong anisotropic growth process can be expected that Ag(I) ions may be selectively adsorbed and be sequentially reduced at the {100} facets of Au NPs, followed by diffusion and accumulation of Au atoms from other part of the cluster to the Ag-containing facets to bury them into the bulk. Accordingly, the reduction rate of Ag(I) is a key step during the growth of Au NWs. If the rate is too high, Ag atoms may not be incorporated into the bulk quickly enough at the very active {100} facets and other Ag(I) ions or even reduced Ag atoms may prefer to adsorb on other facets of gold NPs, leading to the failure of anisotropic growth of Au NWs. On the other hand, the preparation time would be too long if the reduction rate is too low.

To verify the growth mechanism suggested by DFT calculations, the prepared Au NWs were further characterized by XPS (Supplementary Fig. S10). It can be clearly seen that only the signal of Au can be detected although the Au/Ag molar ratio was estimated to be 3.56/1 according to ICP-OES (Supplementary Table S1). This may be due to the fact that most of the Ag component is buried in a small portion of large spherical NPs (Supplementary Fig. S2), and the small amount of Ag in the NWs is undetectable by XPS. It should be noted that the initial molar ratio of Au salt/Ag salt of 15 : 5 is essential for the formation of NW structures (Supplementary Fig. S4). Therefore, we have named the formed NWs as Au NWs although the Ag content in the final product is quite high. In addition, the effect of temperature on the morphology of the NWs was explored (Supplementary Fig. S11). At a low temperature of 20°C, NWs can hardly grow because Ag^+ is hard to be reduced. On the other hand, NWs with a non-uniform morphology were formed at a high temperature (60°C). This is again in agreement with the indication from our DFT calculations that at a high temperature, the quick reducing

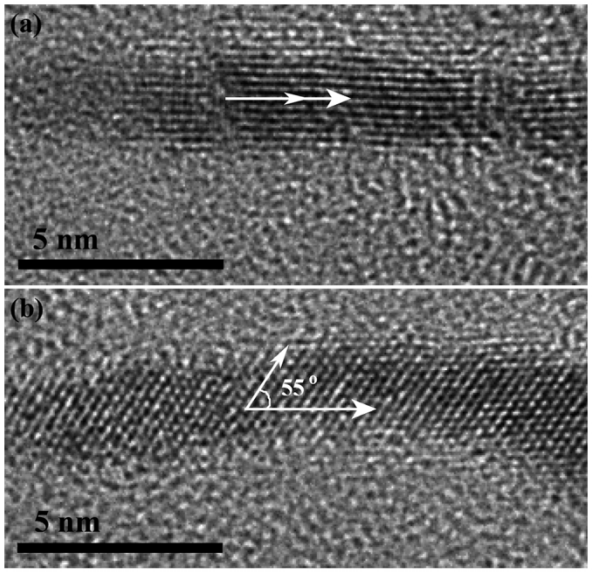

Figure 3 | The growth direction of NWs. High-resolution TEM images of the acetylated NW product showing the {111} crystal facets parallel to (a) or 55° off (b) the growth direction.

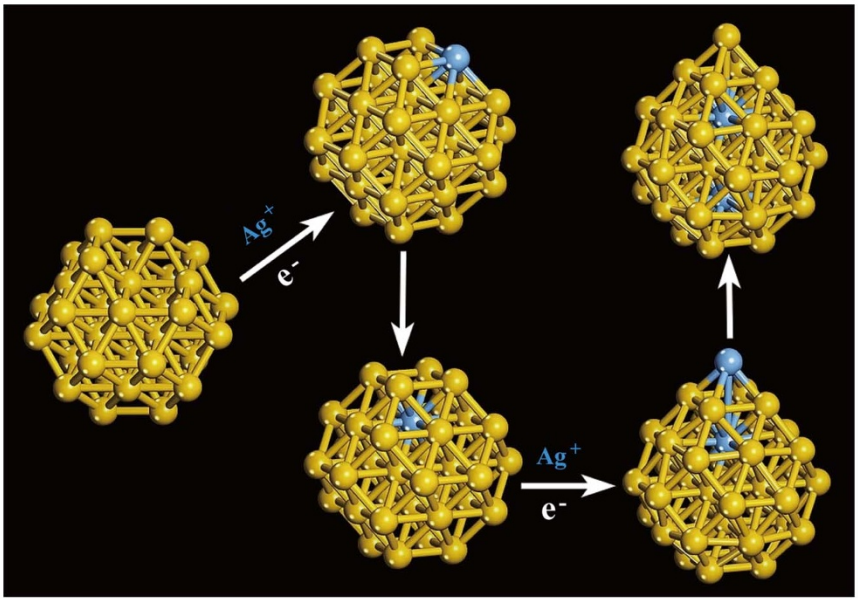

Figure 4 | DFT simulated growth mechanism of the formed NWs. Schematic illustration of the Au NW growth process involving adsorption and mergence of Ag atoms.

of Ag(I) to form Ag(0) makes the deposition of Ag atoms onto the crystal surface of the substrate Au NPs with reduced selectivity.

Furthermore, the use of water as a solvent was found to be essential to generate uniform NWs. We found that the metal reduction rate was dependent on the used solvent in the presence of G5 dendrimers (Supplementary Fig. S12). Due to the lower reduction potential of Ag(I)/Ag pair than that of the Au(III)/Au pair, Ag NPs were not able to be created using dimethylsulfoxide (DMSO), methanol, and water as solvents after 8 h. In contrast, pure Au NPs were able to be formed using all the above solvents in the presence of G5 dendrimers after 8 h, as indicated by the solution color change with time[33]. Being consistent with the shades of color, the reduction rate was highest in DMSO and lowest in water. As indicated from theoretical calculations and experimental analysis, Au NWs containing Ag in the inner area rather than simply mixed Au-Ag NPs can be formed under a low Ag(I) reduction rate after the formation of small Au nuclei NPs. In this sense, such Ag-containing Au NWs should be rather difficult to form in DMSO. This is again confirmed by our further experimental results of the reduction of $AgNO_3$/$HAuCl_4$ in these different solvents. The Ag-Au solution in DMSO became red-purple after 3 h and its color continuously deepened as the time lapsed. By contrast, the solution of the product with the solvents of methanol or water appeared dark, indicating the formation of Au NWs. Our TEM measurements (Supplementary Fig. S13) also confirmed that only spherical particles were formed in DMSO solution, and mixture of NWs and NPs were formed in methanol solution.

Discussion

Ultrathin Au NWs continue to attract a great deal of attention in the scientific community[2,16,19]. Till now the related synthesis protocols are limited in the use of organic solvent, leading to difficulties and complexities in preparation and surface modification of the NWs. In this present work, via a dendrimer-mediated approach, the Au NWs are able to be synthesized in a complete aqueous solution under a mild experimental condition.

The formation process of Au NW structure was first monitored by UV-Vis spectrometry at different time points. The increasing absorbance of the product in the near-infrared region tended to be stable between 36 h and 48 h, suggesting the possible formation of NWs. It is interesting to note that the longitudinal SPR band for the product formed at 8 h and 12 h is not prominent. This could be due to the formation of the mixture of nanorods and spherical NPs (Fig. 1), where the nanorods have a less regular structure when compared with that reported in the literature[34]. Although the quality of the formed NWs seems to be lower than that of the NWs formed through the OA method[2,8], the use of dendrimers as stabilizers allows the generation of NWs in aqueous solution under a mild condition and further surface functionalization of NWs via dendrimer-mediated reaction is possible. The results of ICP-OES analysis indicate that the composition of the particles is Au-dominant at 8 h, which may be due to the fact that the standard reduction potential of the $AuCl_4^-$/Au (0.99 V) is higher than that of the Ag^+/Ag pair (0.80 V), and only a small part of Ag(I) ions are able to be reduced. The Au/Ag molar ratio became close to the molar feed ratio (Au/Ag = 3.00) when the reaction proceeded to 48 h.

It should be noted that the use of $G5.NH_2$ dendrimers is essential to create uniform ultrathin Au NWs. This is largely due to the 3-dimensional globular structure of the G5 dendrimers with highly branched interior that is able to significantly limit the transverse growth of the Au NWs in the presence of Ag(I). In addition, under similar experimental conditions, $G5.NH_2$ possessing much more amine groups than $G3.NH_2$ dendrimers may have stronger reducing capability, leading to the initial generation of smaller Au NPs as seed particles for the growth of ultrathin Au NWs.

Using dendrimers as stabilizers, the surface of the NWs can be easily modified or functionalized, providing many possibilities for their uses in biomedical applications. Acetylation of dendrimer terminal amine has been commonly used to endow the particles to have improved biocompatibility[27,28]. In our study, acetylation of dendrimer surface amines was found to afford the NWs with an increased diameter. This could be ascribed to the fact that the acetylation of some of the dendrimer surface amines that are used to stabilize the Au NWs leads to a further Ostwald ripening process, in agreement with our previous work[21]. The success to form acetylated Au NWs may be extended to prepare biofunctionalized Au NWs by modifying Au NWs via dendrimer-mediated conjugation chemistry, furthering their potential biomedical applications.

Different from the role played by Ag in the formation of Au nanorods, where Ag adsorbs on the sides of the rods and stays on their surface[35], in our study, we proposed a novel growth mechanism

of Au NWs involving a synergic facet-dependent deposition/reduction of Ag(I) and anisotropic migration of Au atoms via DFT calculations (Fig. 4), which was confirmed by experimental results (Supplementary Fig. S10 and Fig. S11).

In summary, ultrathin Au NWs with a diameter of 1.3 nm were readily formed using a dendrimer-mediated hydrothermal approach. A new growth mechanism involving a synergic facet-dependent deposition/reduction of Ag(I) and anisotropic migration of Au atoms is proposed, which is based on DFT calculations. Our data show that the selection of dendrimer stabilizers, reaction solvent and temperature, Au/Ag molar ratio, and reaction time is essential to obtain relatively uniform Au NWs, which are associated with the transverse growth control of Au NWs and the proper reduction rate of Ag(I). This may provide guidance for synthesis of other kinds of NWs in aqueous solution. Moreover, with PAMAM dendrimers as stabilizers instead of the commonly used OA, the scope of preparation and application of Au NWs is remarkably broadened due to the rich dendrimer surface chemistry enabling tunable surface functionalization of the NWs.

Methods

Materials. Ethylenediamine core amine-terminated generation 5 and 3 PAMAM dendrimers (G5.NH_2 and G3.NH_2) were purchased from Dendritech (Midland, MI). Chloroauric acid ($HAuCl_4 \cdot 3H_2O$), silver nitrate ($AgNO_3$), sodium nitrate ($NaNO_3$) and all other chemical agents were obtained from Sinopharm Chemical Reagent Co., Ltd (China) and used as received. Regenerated cellulose dialysis membranes (molecular weight cut-off, MWCO = 10 000) were acquired from Fisher.

Synthesis of Au NWs. An aqueous G5.NH_2 solution (0.192 mM, 5 mL) was pre-heated in a 40°C water bath for 20 min. Under magnetic stirring, $AgNO_3$ solution (58.865 mM, 81.6 μL) was added, followed by addition of an $HAuCl_4$ solution (72.842 mM, 198 μL). The dendrimer/metal salt mixture was kept in the water bath for 2 days. After that, the solution was dialyzed against water for 2 days (2 L, 6 times) using a dialysis membrane with MWCO of 10 000 to remove the excess of reactants and by-products, followed by lyophilization to get Au NWs.

Characterization techniques. UV-Vis spectra were collected using a Lambda 25 UV-Vis spectrometer (Perkin-Elmer, United States). Samples were dissolved in water before the experiments. Transmission electron microscopy (TEM) was performed using a JEOL 2100F analytical electron microscope with an accelerating voltage of 200 kV. An aqueous solution of a sample (1 mg/mL, 5 μL) was dropped onto a carbon-coated copper grid and air dried before measurements. To measure the composition of the products, each sample was dissolved by aqua regia solution (0.2 mL), diluted with water, and then analyzed with inductively coupled plasma-optical emission spectroscopy (ICP-OES) (Leeman Prodigy, USA). ^{1}H NMR spectra were recorded on a Bruker Avance 400 NMR spectrometer. Samples were dissolved in D_2O before measurements. X-ray photoelectron spectrometer (XPS) was performed at base pressure of 5×10^{-8} Pa and test pressure of 2×10^{-6} Pa, using a monochromatic Al rake source at 1486.6 eV and pass energy of 58.7 eV (PHI 5000 Versaprobe microscope).

DFT calculations. Spin-polarization DFT calculations were performed using Perdew-Burke-Ernzerhof (PBE)[36] generalized gradient approximation (GGA) exchange-correlation functional implemented in DMol3 package of Materials Studio (Accerlry Inc.)[37,38]. The localized numerical basis set of double-zeta with polarization functions (DNP 4.4) from DMol3 were utilized with negligible basis set superposition error (BSSE). Density functional semi-core pseudopotentials (DSPP)[39] including mass-velocity and Darwin relativistic corrections were utilized to describe the core-electron interactions of Au and Ag. The global orbital cutoff of 4.5 Å with the self-consistent field (SCF) tolerance of 1.0×10^{-6} Hatree was set to assure the accuracy of calculated energies. During structural optimization, the convergence criteria of maximum energy change, force and displacement were set to 1×10^{-5} Hartree, 2×10^{-3} Hartree/Å, and 5×10^{-3} Å, respectively.

1. Christopher, P. & Linic, S. Shape- and size-specific chemistry of Ag nanostructures in catalytic ethylene epoxidation. *Chemcatchem* **2**, 78–83 (2010).
2. Wang, C., Hu, Y. J., Lieber, C. M. & Sun, S. H. Ultrathin Au nanowires and their transport properties. *J. Am. Chem. Soc.* **130**, 8902–8903 (2008).
3. Wu, B., Heidelberg, A. & Boland, J. J. Mechanical properties of ultrahigh-strength gold nanowires. *Nat. Mater.* **4**, 525–529 (2005).
4. Hong, X., Wang, D. S. & Li, Y. D. Kinked gold nanowires and their SPR/SERS properties. *Chem. Commun.* **47**, 9909–9911 (2011).
5. Liu, Z. & Searson, P. C. Single nanoporous gold nanowire sensors. *J. Phys. Chem. B* **110**, 4318–4322 (2006).
6. Yogeswaran, U. & Chen, S.-M. A review on the electrochemical sensors and biosensors composed of nanowires as sensing material. *Sensors* **8**, 290–313 (2008).
7. Wang, Q.-Q. *et al.* Highly efficient avalanche multiphoton luminescence from coupled Au nanowires in the visible region. *Nano Lett.* **7**, 723–728 (2007).
8. Halder, A. & Ravishankar, N. Ultrafine single-crystalline gold nanowire arrays by oriented attachment. *Adv. Mater.* **19**, 1854–1858 (2007).
9. Pei, L. H., Mori, K. & Adachi, M. Formation process of two-dimensional networked gold nanowires by citrate reduction of AuCl4- and the shape stabilization. *Langmuir* **20**, 7837–7843 (2004).
10. Giersig, M., Pastoriza-Santos, I. & Liz-Marzan, L. M. Evidence of an aggregative mechanism during the formation of silver nanowires in N, N-dimethylformamide. *J. Mater. Chem.* **14**, 607–610 (2004).
11. Kim, F., Sohn, K., Wu, J. S. & Huang, J. X. Chemical synthesis of gold nanowires in acidic solutions. *J. Am. Chem. Soc.* **130**, 14442–14443 (2008).
12. Liu, X. G., Wu, N. Q., Wunsch, B. H., Barsotti, R. J., Jr. & Stellacci, F. Shape-controlled growth of micrometer-sized gold crystals by a slow reduction method. *Small* **2**, 1046–1050 (2006).
13. Bai, H. Y., Xu, K., Xu, Y. J. & Matsui, H. Fabrication of an nanowires of uniform length and diameter using a monodisperse and rigid biomolecular template: Collagen-like triple helix. *Angew. Chem.-Int. Edit.* **46**, 3319–3322 (2007).
14. Kim, J. U., Cha, S. H., Shin, K., Jho, J. Y. & Lee, J. C. Preparation of gold nanowires and nanosheets in bulk block copolymer phases under mild conditions. *Adv. Mater.* **16**, 459–464 (2004).
15. Cross, C. E., Hemminger, J. C. & Penner, R. M. Physical vapor deposition of one-dimensional nanoparticle arrays on graphite: Seeding the electrodeposition of gold nanowires. *Langmuir* **23**, 10372–10379 (2007).
16. Huo, Z. Y., Tsung, C.-K., Huang, W. Y., Zhang, X. F. & Yang, P. D. Sub-two nanometer single crystal Au nanowires. *Nano Lett.* **8**, 2041–2044 (2008).
17. Lu, X. M., Yavuz, M. S., Tuan, H.-Y., Korgel, B. A. & Xia, Y. N. Ultrathin gold nanowires can be obtained by reducing polymeric strands of oleylamine-AuCl complexes formed via aurophilic interaction. *J. Am. Chem. Soc.* **130**, 8900–8901 (2008).
18. Pazos-Perez, N. *et al.* Synthesis of flexible, ultrathin gold nanowires in organic media. *Langmuir* **24**, 9855–9860 (2008).
19. Xu, J. *et al.* Mechanical nanosprings: Induced coiling and uncoiling of ultrathin Au nanowires. *J. Am. Chem. Soc.* **132**, 11920–11922 (2010).
20. Feng, H. J. *et al.* Simple and rapid synthesis of ultrathin gold nanowires, their self-assembly and application in surface-enhanced Raman scattering. *Chem. Commun.* 1984–1986 (2009).
21. Liu, H. *et al.* Dendrimer-mediated synthesis and shape evolution of gold-silver alloy nanoparticles. *Colloid Surf. A-Physicochem. Eng. Asp.* **405**, 22–29 (2012).
22. Wilson, O. M., Scott, R. W. J., Garcia-Martinez, J. C. & Crooks, R. M. Synthesis, characterization, and structure-selective extraction of 1-3-nm diameter AuAg dendrimer-encapsulated bimetallic nanoparticles. *J. Am. Chem. Soc.* **127**, 1015–1024 (2005).
23. Peng, C. *et al.* PEGylated dendrimer-entrapped gold nanoparticles for in vivo blood pool and tumor imaging by computed tomography. *Biomaterials* **33**, 1107–1119 (2012).
24. Wen, S. *et al.* Multifunctional dendrimer-entrapped gold nanoparticles for dual mode CT/MR imaging applications. *Biomaterials* **34**, 1570–1580 (2013).
25. Chen, Q. *et al.* Targeted CT/MR dual mode imaging of tumors using multifunctional dendrimer-entrapped gold nanoparticles. *Biomaterials* **34**, 5200–5209 (2013).
26. Shi, X., Sun, K. & Baker, J. R., Jr. Spontaneous formation of functionalized dendrimer-stabilized gold nanoparticles. *J. Phys. Chem. C* **112**, 8251–8258 (2008).
27. Shi, X. *et al.* Dendrimer-entrapped gold nanoparticles as a platform for cancer-cell targeting and Imaging. *Small* **3**, 1245–1252 (2007).
28. Shi, X., Wang, S. H., Sun, H. P. & Baker, J. R., Jr. Improved biocompatibility of surface functionalized dendrimer entrapped gold nanoparticles. *Soft Matter* **3**, 71–74 (2007).
29. Mulvaney, P., Giersig, M. & Henglein, A. Electrochemistry of multilayer colloids: Preparation and absorption spectrum of gold-coated silver particles. *J. Phys. Chem.* **97**, 7061–7064 (1993).
30. Hong, X. *et al.* Ultrathin Au–Ag bimetallic nanowires with Coulomb blockade effects. *Chem. Commun.* **47**, 5160–5162 (2011).
31. Wang, C. & Sun, S. H. Facile synthesis of ultrathin and single-crystalline Au nanowires. *Chem.-Asian J.* **4**, 1028–1034 (2009).
32. Liu, X. Y. *et al.* Synthesis of thermally stable and highly active bimetallic Au–Ag nanoparticles on inert supports. *Chem. Mater.* **21**, 410–418 (2008).
33. Shen, M. W., Sun, K. & Shi, X. Hydroxylated dendrimer-stabilized gold and silver nanoparticles: Spontaneous formation, characterization, and surface properties. *Curr. Nanosci.* **6**, 307–314 (2010).
34. Smith, D. K., Miller, N. R. & Korgel, B. A. Iodide in CTAB prevents gold nanorod formation. *Langmuir* **25**, 9518–9524 (2009).
35. Orendorff, C. J. & Murphy, C. J. Quantitation of metal content in the silver-assisted growth of gold nanorods. *J. Phys. Chem. B* **110**, 3990–3994 (2006).
36. Perdew, J. P., Burke, K. & Ernzerhof, M. Generalized gradient approximation made simple. *Phys. Rev. Lett.* **77**, 3865–3868 (1996).
37. Delley, B. An all-electron numerical method for solving the local density functional for polyatomic molecules. *J. Chem. Phys.* **92**, 508–517 (1990).
38. Delley, B. From molecules to solids with the DMol approach. *J. Chem. Phys.* **113**, 7756–7764 (2000).

39. Delley, B. Hardness conserving semilocal pseudopotentials. *Phys. Rev. B* **66**, 155125 (2002).

Acknowledgments

This research is financially supported by the National Natural Science Foundation of China (21273032) and the Fund of the Science and Technology Commission of Shanghai Municipality (11 nm0506400). The ECUST group thanks financial support from National Basic Research Program (2011CB808505) and Shanghai Rising-Star Program (12QH1400700). Computing time in the National Super Computing Center in Jinan is acknowledged. H. L. thanks the Innovation Funds of Donghua University Doctorate Dissertation of Excellence (105-06-0019023). X. S. gratefully acknowledges the Fundaçãopara a Ciência e a Tecnologia (FCT) for funding through the project PTDC/CTM-NAN/1748/2012.

Author contributions

X.S. contributed to the design of the experiment, analysis of the data and writing the manuscript. X.G. contributed to the simulation part of the paper and writing of the manuscript. H.L. performed the synthesis and characterization of the materials and wrote the draft of the manuscript. X.C. performed the simulation analysis. J.Y. assisted the TEM analysis. H.L. and X.C. contributed equally to this work.

Additional information

Supplementary information accompanies this paper at http://www.nature.com/scientificreports

Competing financial interests: The authors declare no competing financial interests.

How to cite this article: Liu, H., Cao, X., Yang, J., Gong, X. & Shi, X. Dendrimer-mediated hydrothermal synthesis of ultrathin gold nanowires. *Sci. Rep.* **3**, 3181; DOI:10.1038/srep03181 (2013).